Materials Science-Poland, 36(4), 2018, pp. 547-552
http://www.materialsscience.pwr.wroc.pl/
DOI: 10.2478/msp-2018-0088

Synthesis of NiO nanoparticles by sol-gel technique

ZOHRA NAZIR KAYANI[1,*], MAHEK ZAHEEN BUTT[1], SAIRA RIAZ[2], SHAHZAD NASEEM[2]

[1]Physics Department, Lahore College for Women University, Lahore-54000, Pakistan
[2]Center for Solid State Physics, University of the Punjab, Lahore-54590, Pakistan

NiO nanoparticles were fabricated by sol-gel route using ammonium hydroxide and nickel nitrate as precursors. The NiO nanoparticles were calcinated at 400 °C and 1000 °C. The nanoparticles were characterized by X-ray diffraction (XRD), Fourier transform infrared spectroscopy (FT-IR), vibrating sample magnetometer (VSM), thermogravimetry analysis/differential thermal analysis (TGA/DTA). The structural properties were evaluated by X-ray diffraction (XRD). XRD confirmed the formation of well-crystallized and high purity NiO phase. The XRD showed that the peaks were sharpened and the crystallite size increased as the calcination temperature increased. The average crystallite size ranged from 12 nm to 20 nm, when calcined at temperatures 400 °C and 1000 °C, respectively. Fourier transform infrared spectroscopy (FT-IR) revealed the chemical composition and confirmed the formation of NiO nanoparticles. The nanoparticles showed paramagnetic behavior.

Keywords: *NiO; nanoparticles; calcination; crystallite size; FT-IR*

1. Introduction

Nickel oxide is an antiferromagnetic transition metal oxide, which is a wide gap p-type semiconductor [1]. It is an interesting material because of its chemical stability as well as optical, electrical and magnetic properties. Its nanoparticles are used in electrochromic devices [2], smart windows [3], optical fibers [4], gas sensors [5], solar thermal absorbers [6], batteries [7], transparent conducting layers [8]. Numerous techniques, such as chemical precipitation [9, 10], magnetron sputtering [10], and sol-gel [11] have been used to fabricate NiO nanoparticles. Among different techniques for controlled synthesis, sol-gel technique was used to synthesize crystalline and impurity free NiO nanoparticles. Jahromi et al. [12] showed that crystallite size of NiO nanoparticles increased on annealing. Alagiri et al. [11] synthesized NiO nanoparticles with super-paramagnetic behavior, which showed the optical band gap of 3.51 eV. In this project, low band gap has been achieved as compared to the band gap of NiO nanoparticles reported in the literature [11]. Doping of different materials has been done by different researchers to enhance the properties of NiO nanoparticles [13]. Crystalline phases associated with crystal planes were evaluated by X-ray diffraction (XRD). The structure and chemical bonding of the nanoparticles were studied by Fourier transform infrared spectroscopy (FT-IR). Thermal properties of the NiO nanoparticles were examined by thermal gravimetric analysis/differential thermal analysis (TGA/DTG). Magnetic properties were studied by vibrating scale magnetometer (VSM) and optical properties were evaluated by UV-Vis-IR spectrophotometer.

2. Experimental

100 mL of 2 M NH_4OH solution was added dropwise into 50 mL of 0.5 M Ni $(NO_3)_2 \cdot 6H_2O$ solution which was stirred by a magnetic stirring apparatus at 100 °C for four hours. The sol was kept at room temperature for 24 hours for aging. The prepared light-green suspension was centrifuged and then calcined at 400 °C and 1000 °C for 2 hours.

X-ray diffraction study with a Bruker D8, Germany, (CuKα radiation $\lambda = 1.54060$ Å) was performed for structural characterization of the nanoparticles before and after annealing in a furnace. Diffraction angle was adjusted from 20°

*E-mail: zohrakayani@yahoo.com

to 80° with a step of 0.02°. Particle size was evaluated using Malvern Mastersizer 3000 particle size analyzer.

The infrared spectra were measured in the range of 400 cm^{-1} to 4000 cm^{-1} by FT-IR Model M 2000 Midac, USA. Thermal properties TGA/DTA and DSC were studied using SDT Q 600 thermogravimetric analyzer. The temperature was increased from room temperature to 1000 °C with an increment of 10 °C/min in air. Magnetic properties were analyzed by Lakeshore 7407 vibrating sample magnetometer VSM. Optical transmission spectra of the nanoparticles were measured by UV-Vis spectrophotometer (UV-Vis, HITACHI U-2800) in the wavelength range of 200 nm to 900 nm.

3. Results and discussion

3.1. FT-IR study

The FT-IR spectrum in Fig. 1 shows that nickel oxide nanoparticles calcined at 400 °C have a broad absorption band centered at around 3843 cm^{-1} and 3287 cm^{-1} which could be due to the O–H stretching vibrations. The band at 1627 cm^{-1} can be attributed to the bending vibrations of water molecules. The band at 1385 cm^{-1} is due to the presence of C–O bonds [14]. The strong band at 614 cm^{-1} and 419 cm^{-1} corresponds to vibrations of Ni–O bonds. Nickel oxide nanoparticles calcined at 1000 °C have almost the same pattern with a slight change in the vibration of Ni–O bond. The peaks are shifted to 620 cm^{-1} and 471 cm^{-1}. The FT-IR spectrum at 400 °C shows the characteristics peaks at 419 cm^{-1}, 614 cm^{-1}, 1385 cm^{-1}, 1627 cm^{-1}, 3287 cm^{-1}, 3843 cm^{-1}. The bands at 419 cm^{-1} and 614 cm^{-1} suggest the presence of NiO. Despite annealing, the nanoparticles reveal traces of water (peaks at 1627 cm^{-1}, 3287 cm^{-1} and 3843 cm^{-1}). There is no peak indicating the presence of ammonia as the nanoparticles were washed with high purity water. This indicates that the sample has no traces of impurity. As Fig. 1 shows, the annealing at 1000 °C did not alter the chemical composition of NiO nanoparticles but only caused peaks shifting to 620 cm^{-1} and 471 cm^{-1}.

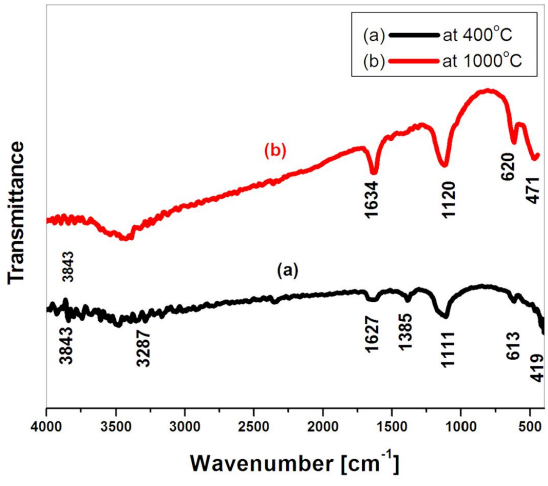

Fig. 1. FT-IR patterns of nickel oxide nanoparticles obtained at annealing temperatures of (a) 400 °C, and (b) 1000 °C.

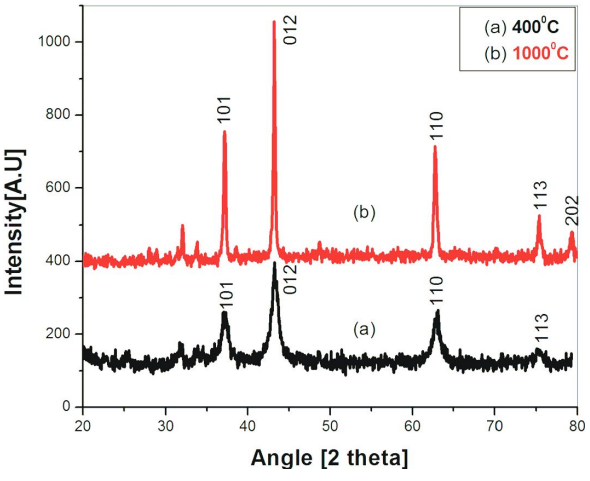

Fig. 2. XRD patterns of NiO nanoparticles annealed at (a) 400 °C, and (b) 1000 °C.

3.2. Structural studies

Structural analysis of the NiO nanoparticles was performed using CuKα radiation source of a wavelength $\lambda = 1.54060$ Å and the diffraction patterns were studied by changing diffraction angle in the range of 20° to 80°. Fig. 2 shows the XRD patterns of NiO nanoparticles synthesized by sol-gel technique and annealed at temperatures of 400 °C and 1000 °C, respectively. It can be stated from the XRD pattern that all the samples are polycrystalline and have NiO

hexagonal structure. High temperature annealing carried out at 1000 °C enhanced the formation of crystalline structure in the nanoparticles, as evidenced by the presence of diffraction peaks in Fig. 2. The d-values of the XRD patterns were compared with JCPDS Card No. 22-1189. Good agreement was observed between JCPDS Card d-values and calculated d-values, which confirms that the nanoparticles of NiO have hexagonal structure. It can be observed that by increasing the annealing temperature from 400 °C up to 1000 °C, the peaks became appreciably sharpened which indicates that a growth in the crystallite size of NiO has taken place.

The average crystallite sizes D of nickel oxide nanoparticles were calculated by Debye-Scherer equation [15] using full width at half maximum:

$$D = k\lambda/\beta cos\theta \qquad (1)$$

where D is the crystallite size, β is the broadening of the diffraction line measured at its half maximum intensity (FWHM), k is the Scherer constant of the order of 0.9 related to crystallite shape and λ is the wavelength of the X-ray beam. Crystallite size of NiO nanoparticles increased from 12.4 nm at 400 °C to 20.7 nm at 1000 °C, while dislocation density decreased from 6.5×10^{-3} nm^{-2} to 2.3×10^{-3} nm^{-2} with the increase in annealing temperature. Crystallite size of the nanoparticles confirms the formation of the nanocrystalline structure. In NiO nanoparticles there are several dangling bonds related to nickel-oxygen defects at the grain boundaries. These defects lead to the merging process leading to forming bigger NiO grains, i.e. coalescence of the grains at elevated annealing temperature [16, 17] results in increased crystallite size. In fact, crystallinity of NiO thin films is enhanced at elevated annealing temperatures. High annealing temperature supplies energy to crystallites which transfers them to stable equilibrium sites, leading to the enhancement in crystallinity and degree of orientation of the NiO films.

Particle sizes of the NiO nanoparticles were analyzed using particle size analyzer and they turned out to be 20 nm for nanoparticles annealed at 400 °C and 32 nm after annealing at 1000 °C. They showed the same trend as the crystallite size obtained by Scherrer relation and increased after annealing at high temperature. Crystallite size of the nanoparticles is small as compared to the values reported in the literature [18–20].

3.3. TGA/DTA analysis

TGA and DTA curves of the nickel oxide are shown in Fig. 3. Three weight losses can be observed in the TGA curve (a) at 60 °C (I), 660 °C (II), and 760 °C (III), The weight loss at 660 °C and 760 °C is accompanied by a sharp DTA peak (b). The minor weight loss (I) observed at 60 °C is due to desorption of water. The second weight loss step (II) at 660 °C is attributed to impurities or adsorbents of NiO. The weight loss at 760 °C (III, broad peak at DTA) is connected with creation of defects in the NiO powder. These defects are associated with the loss of oxygen, enhancing the formation of oxygen vacancies. The weight loss is due to thermal decomposition or dehydration of $Ni(OH)_2$ to form NiO particles. Similar observation of weight loss of NiO was reported by Nassar et al. [21].

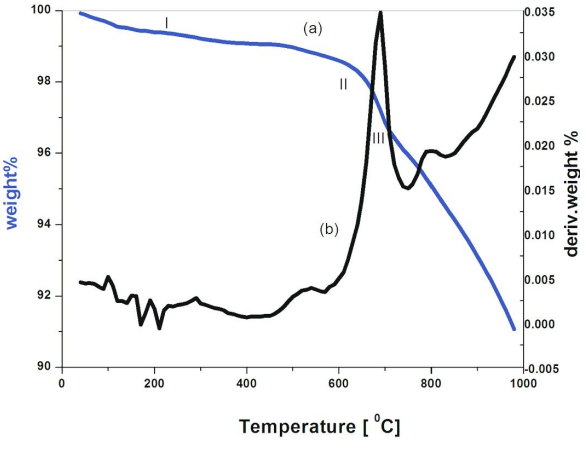

Fig. 3. TGA/DTA curves of nickel oxide nanoparticles at annealing temperatures of 400 °C and 1000 °C.

3.4. Optical properties

Optical transmittance spectra of NiO nanoparticles obtained at different annealing temperatures are presented in Fig. 4. Optical transmittance

of NiO nanoparticles shows strong dependence on the annealing temperatures. The sample annealed at 400 °C has lower transmittance than the one annealed at 1000 °C. A rapid decrease in transmission, which is termed as fundamental absorption band edge of NiO, is observed at wavelength of ∼411 nm for nanoparticles annealed at 400 °C and 395 nm for nanoparticles annealed at 1000 °C. The value of band gap increased from 3.02 eV to 3.14 eV as the annealing temperature of NiO nanoparticles increased from 400 °C to 1000 °C [22–24]. The transmission increased at elevated annealing temperature due to improvement in crystalline microstructure and reduced defect scattering. As the annealing temperature increased, grain size and band gap values increased. Thus, it can be stated that the band gap is dependent directly on the grain size. Increasing the annealing temperature, hence, the grain size, causes that Ni^{3+} ions are removed [25] and the defects are reduced, resulting in the observed shift to the shorter wavelengths. The removal of Ni^{3+} ions reduces density of the localized states tails in the band structure, hence, the width of localized states, and increases the optical band gap energy [26].

The band gap obtained in this project is less than the values reported in the literature [20, 27]. These small band gap materials find application in quantum devices, infrared sensors and detectors [28] and spintronics [29].

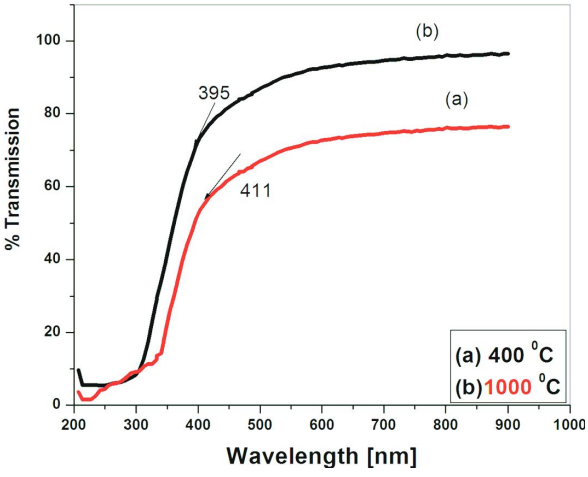

Fig. 4. Percentage of transmission through NiO nanoparticles annealed at (a) 400 °C, and (b) 1000 °C.

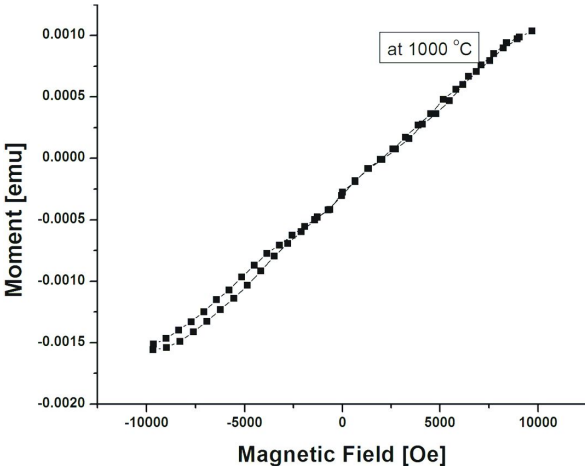

Fig. 5. Magnetic properties of NiO nanoparticles after annealing at 1000 °C.

3.5. Magnetic properties

M–H behavior of the prepared NiO nanoparticles is shown in Fig. 5.

The magnetization has not saturated up to the maximum applied field of 10 kOe. Magnetization increased with increasing field showing no sign of saturation in the field range studied (±10 kOe).The M–H curve does not show any significant hysteresis and retentivity. Magnetization studies revealed nearly temperature independent paramagnetism. It can be seen in Fig. 5 that the coercive field is not zero for the nanoparticles. The coercivity of the nanoparticles annealed at 1000 °C is 49 Oe. The saturation magnetization Ms and retentivity Mr of the NiO nanoparticles were found to be 4.326×10^{-3} emu/g and 3.828×10^{-5} emu/g, respectively. NiO nanoparticles have the squareness ratio of 8.84×10^{-3}. Susceptibility χ of the paramagnetic NiO nanoparticles turned out to be 8.866×10^{-5}. From Fig. 5 it is evident that the magnetization of NiO nanoparticles shows more or less linear dependence on the applied magnetic field. Therefore, NiO nanoparticles show paramagnetic behavior [24]. If the size of metal nanoparticles is decreased below their critical diameter of approximately 55 nm, the nanoparticles become single magnetic domains [30, 31]. Ferromagnetic

behavior is observed when nanoparticles have the grain size greater than critical domain size, otherwise smaller nanoparticles show paramagnetic behavior. XRD analysis showed the grain size of 20.7 nm when the nanoparticles were annealed at 1000 °C that is why the nanoparticles are paramagnetic in nature. The magnetic measurements clearly show the existence of paramagnetism in NiO nanoparticles, which may be due to the presence of uncompensated Ni ions at the surface of the particles.

NiO is originally antiferromagnetic (AFM) but nanoparticles of NiO can show magnetic properties (paramagnetic, ferromagnetic or antiferromagnetic) at nanoscale depending on crystallite size, annealing temperature, surface magnetization and existence of ferromagnetic Ni clusters. The nanoparticles can be ferromagnetic or paramagnetic depending upon the magnetic retort of disordered spins. This disorder is more prominent in smaller nanoparticles because of defects and dangling bonds on the surface. In this project, the crystallite size enhanced with an increase in annealing temperature which suggests the decrement of Ms with increasing annealing temperature owing to the reduced surface to volume ratio and an increased probability of paramagnetism of the nanoparticle. Ferromagnetism in NiO nanoparticles may be due to Ni clusters [32] but it is still under research as it is crucial for applications. Ferromagnetism [33] and antiferromagnetism in NiO nanoparticles have been reported in the literature [33–35]. For biological and biomedical applications, nanoparticles which show reversible magnetic characteristics at room temperature, i.e. paramagnetic, are most suitable [36], while for data storage applications, particles should have a stable, switchable magnetic state which remains unaffected by temperature variations in order to represent information bits.

4. Conclusions

Nanocrystalline nickel oxide nanoparticles were synthesized by inexpensive sol-gel method. The NiO nanoparticles were annealed at temperatures of 400 °C and 1000 °C. The XRD results showed that the NiO nanoparticles have a good nanocrystalline hexagonal structure. Their grain size increased from 12.4 nm to 20.7 nm with increasing the annealing temperature from 400 °C to 1000 °C. Optical transmission studies showed low absorbance in IR and visible regions with a band gap 3.02 eV (at 400 °C) which was increased to 3.14 eV (at 1000 °C). This increase in the band gap is due to the increase in defect levels.

References

[1] KAMAL H., ELMAGHRABY K.E., ALI A.S., ABDEL-HADY K., *J. Cryst. Growth,* 262 (2004), 424.

[2] HE J., LINDSTROM H., HAGFELDT A., LINDQUIST E.S., *J. Phys. Chem. B,* 103 (1999), 8940.

[3] YOSHIMURA K., MIKI T., TANEMURA S., *Jpn. J. Appl. Phys.,* 34 (1995), 2440.

[4] LIU K., ANDERSON M., *J. Electrochem. Soc.,* 143 (1966), 124.

[5] HOTOVY I., REHACEK V., SICILIANO P., CAPONE S., SPIESS L., *Thin Solid Films,* 418 (2002), 9.

[6] COOK G.J., KOFFYBERG P.F., *Sol. Energ. Mater.,* 10 (1984), 55.

[7] MAKKUS C.R., HEMMES K., WIT D.W.H.J., *J. Electrochem. Soc.,* 141 (1994), 3429.

[8] CHAN M.I., HSU Y.T., HONG C.F., *Appl. Phys. Lett.,* 81 (2002), 1899.

[9] DERAKHSHI M., JAMALI T., ELYASI M., BIJAD M., SADEGHI R., KAMALI A., NIAZAZARI K., SHAHMIRI R.M., BHARI A., MOKHTARI S., *Int. J. Electrochem. Sc.,* 8 (2013), 8252.

[10] KHANSARI A., ENHESSARI M., NIASARI S.M., *J. Clust. Sci.,* 24 (2013), 289.

[11] ALAGIRI M., PONNUSAMY S., MUTHAMIZHCHELVAN C., *J. Mater. Sci. Mater. El.,* 23 (2012), 728.

[12] JAHROMI P.S., HUANG M.N., MUHAMAD R.M., LIM N.H., *Ceram. Int.,* 39 (2013), 3909.

[13] MALLICK P., RATH C., BISWAL R., MISHRA C.N., MISHRA C.N., *Indian J. Phys.,* 83 (2009), 517.

[14] ALIAS S.S., ISMAIL B.A., MOHAMAD A.A., *J. Alloy. Compd.,* 499 (2010), 231.

[15] JENKINS R., SNYDER L.R., *Introduction to X-ray Powder Diffractometry*, John Wiley & Sons, New Jersey, 1996.

[16] COMINI E., FAGLIA G., SBERVEGLIERI G., PAN Z., WANG L.W., *Appl. Phys. Lett.,* 81 (2012), 1869.

[17] ALIAHMAD M., NOORI M., *Indian J. Phys.,* 87 (2013), 43.

[18] ZORKIPLI M.N.N., KAUS M.H.N., MOHAMAD A.A., *Procedia Chem.,* 19 (2016), 626.

[19] GANDHI C.A., CHENG H.-Y., CHANG Y.-M., LIN G.J., *Mater. Res. Express,* 3 (3) (2016), 035017.

[20] EL-KAMRAY M., NAGY N., EL-MEHASSEB I., *Mat. Sci. Semicon. Proc.,* 16 (6) (2013), 1747.

[21] NASSAR N.N., HASSAN A., ALMAO P.P., *Appl. Catal. A-Gen.,* 462 – 463 (2013), 116.

[22] KALAM A., AL-SHIHRI S.A., SHAKIR M., EL-BINDARY A.A., YOUSEF S.E., DU G., *Synth. React. Inorg. M.,* 41 (2011), 1324.
[23] AL-SEHEMI G.A., AL-SHIHRI S.A., KALAM S.A., DU G., AHMAD T., *J. Mol. Struct.,* 1058 (2014), 56.
[24] ANANDAN K., RAJENDRAN V., *IJNN.,* 2 (4) (2012), 24.
[25] MENDOZA-GALVAN A., VIDALES-HURTADO A., LOPEZ-BELTRAN M.A., *Thin Solid Films,* 517 (2009), 3115.
[26] MAKHLOUF A.S., KASEEM A.M., ABDEL-RAHIM A.M., *Optoelectron. Adv. Mat.,* 4 (2010), 1562.
[27] ZATSEPIN F.A., KUZNETSOVA A.Y., SOKOLOV I.V., *J. Lumin.,* 183 (2017), 135.
[28] MCGILL C.T., COLLINS A.D., *Semicond. Sci. Tech.,* 8 (1993), Sl.
[29] WANG X.-L., DOU X.S., ZHANG C., *NPG Asia Mater.,* 2 (2010), 31.
[30] AHMED T., RAMANUJACHARY V.K., LOFLAND E.S., GANGULI K.A., *Solid State Sci.,* 8 (2006), 425.
[31] LU A.H., SALABAS E.L., SCHUTH F., *Angew. Chem. Int. Edit.,* 46 (2007), 1222.
[32] MOURDIKOUDIS S., SIMEONIDIS K., VILALTA-CLEMENTE A., TUNA F., TSIAOUSSIS I., ANGELAKERIS M., DENDRINOU-SAMARA C., KALOGIROU O., *J. Magn. Magn. Mater.,* 321 (2009), 2723.
[33] GANDHI C.A., LIN G.J., *J. Magn. Magn. Mater.,* 424 (2017), 221.
[34] LIMA A.T.A., DANTAS L.A., ALMEIDA S.N., *J. Magn. Magn. Mater.,* 425 (2017), 72.
[35] NADEEM K., ULLAH A., MUSHTAQ M., KAMRAN M., HUSSAIN S.S., MUMTAZ M., *J. Magn. Magn. Mater.,* 417 (2016), 6.
[36] DAVE S.R., GAO X.H., *WIRES Nanomed. Nanobi.,* 1 (2009), 583.

Received 2016-09-29
Accepted 2018-09-18